

Cell-based assays

Colorimetric assays

Prof. Dr. Andrei Leitao

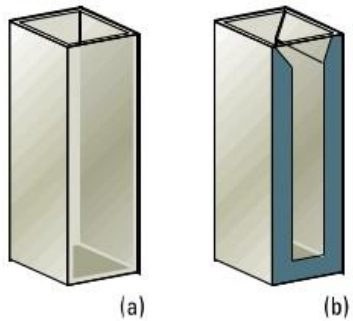
# Electromagnetic spectrum

## Colors & Wavelengths

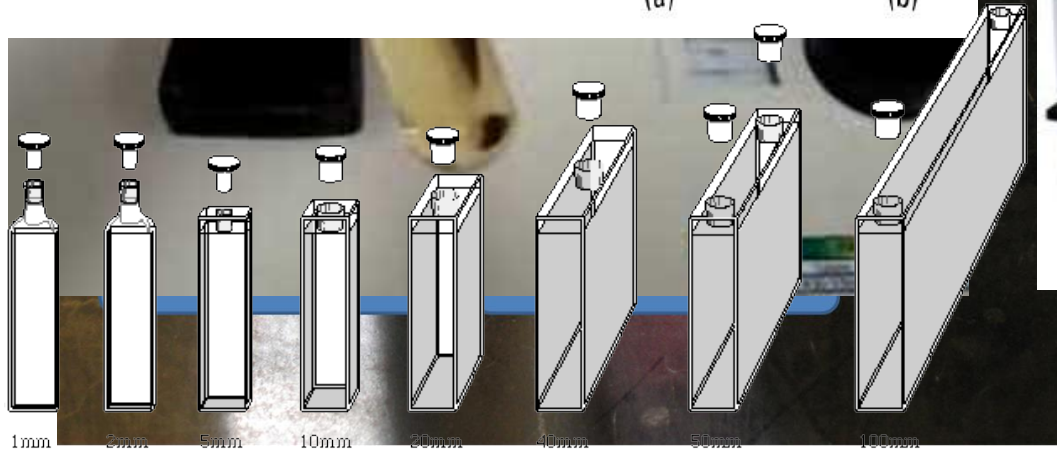
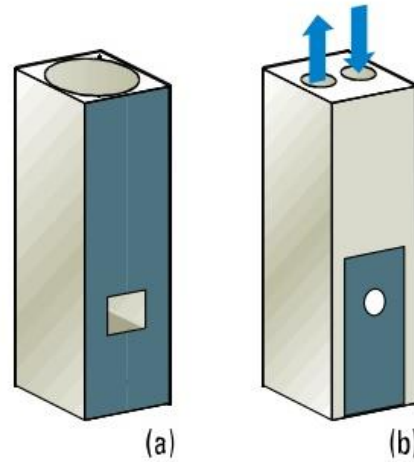
	COLOR	WAVELENGTH ( $\lambda$ in nm)	
of t 1	Violet	380 – 435	
	Blue	436 – 480	
	Greenish-blue	481 – 490	
	Bluish-green	491 – 500	
	Green	501 – 560	
	Yellowish-green	561 – 580	
	Yellow	581 – 595	
	Orange	596 – 650	
	Red	651 – 780	

# Spectrophotometers

## Cell Types I



## AND II



[http://www.umich.edu/~chem125/softchalk/Exp2\\_Final\\_2/Exp2\\_Final\\_2\\_print.html](http://www.umich.edu/~chem125/softchalk/Exp2_Final_2/Exp2_Final_2_print.html)

<https://www.youtube.com/watch?v=Rem9KkolKBI>

<http://www.news-medical.net/Multiskan-GO-Microplate-Spectrophotometer-from-Thermo-Scientific>

[http://www.starnacells.com/d\\_cells\\_s/rect/T021.html](http://www.starnacells.com/d_cells_s/rect/T021.html)

<http://www.nanodrop.com/productnd2000overview.aspx>

# Inside the spectrophotometer

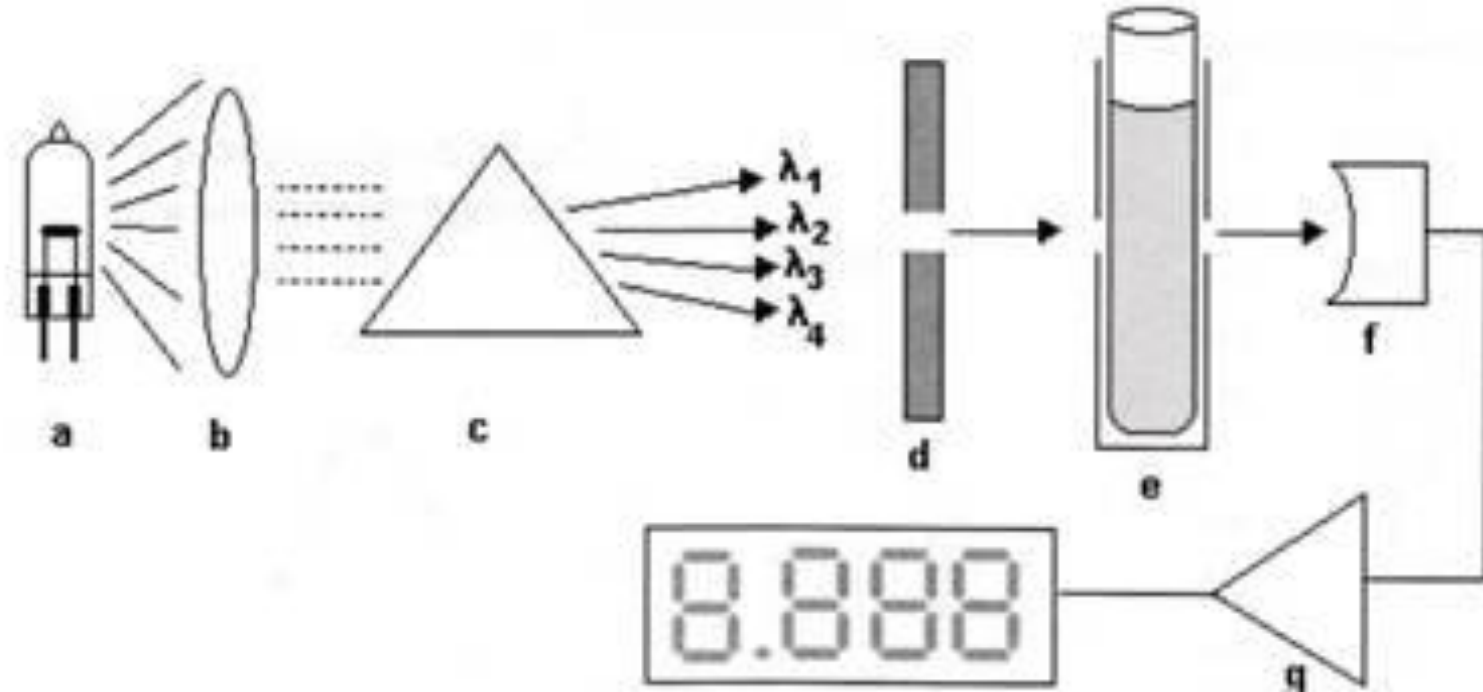


**Figure.** Optical scheme of the main spectrophotometer components.

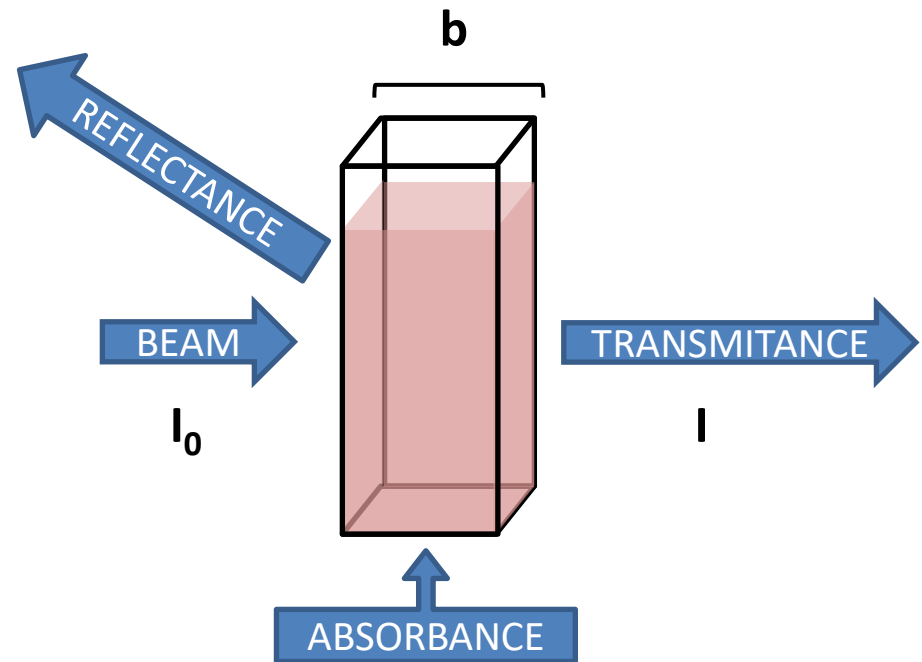
(a) Light source, (b) Colimator, (c) Prism, (d)  $\lambda$  selector slit, (e) sample compartment with cubette, (f) photoelectric cell, (g) amplifier.

# Colorimetric assays –basic principles

Lambert - Beer's Law

$$A = \log \frac{I_0}{I} = \epsilon bc$$

$\epsilon$  = molar absorptivity  
 $b$  = sample's path length  
 $c$  = concentration



# Colorimetric assays –basic principles

Lambert - Beer's Law

$$A = \log \frac{I_0}{I} = \epsilon bc$$

$\epsilon$  = molar absorptivity  
 $b$  = sample's path length  
 $c$  = concentration

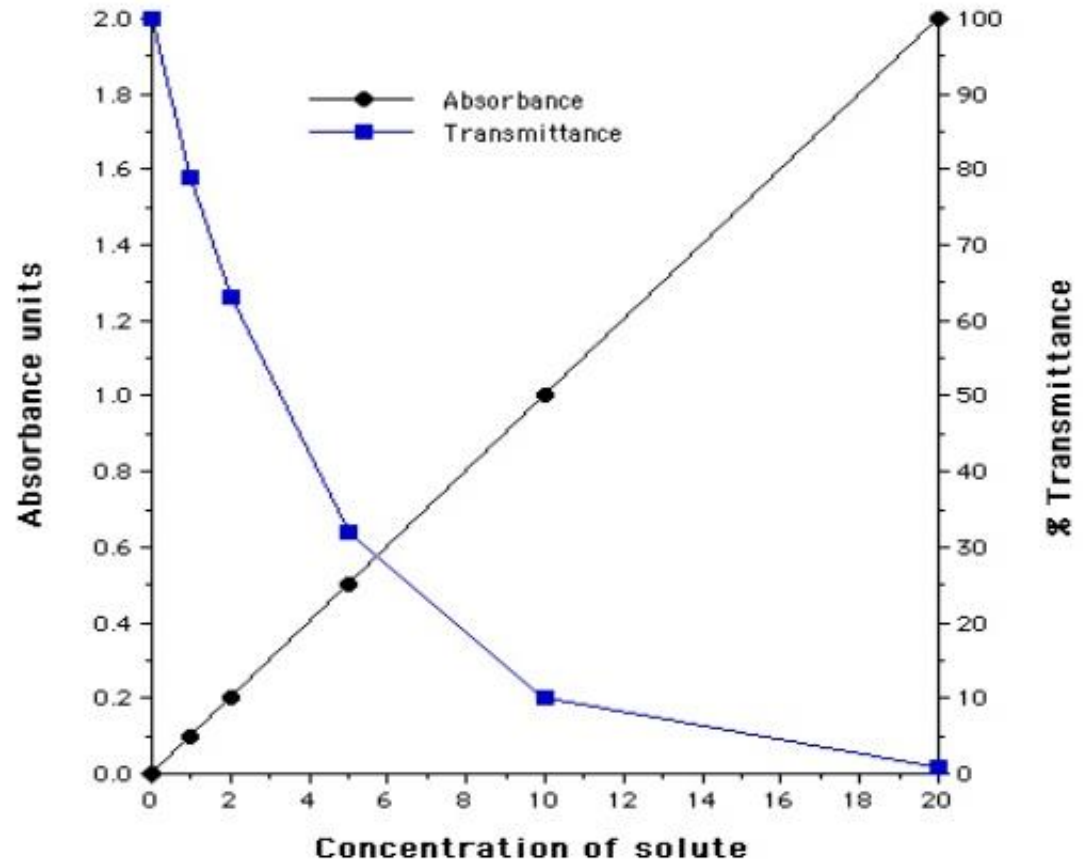
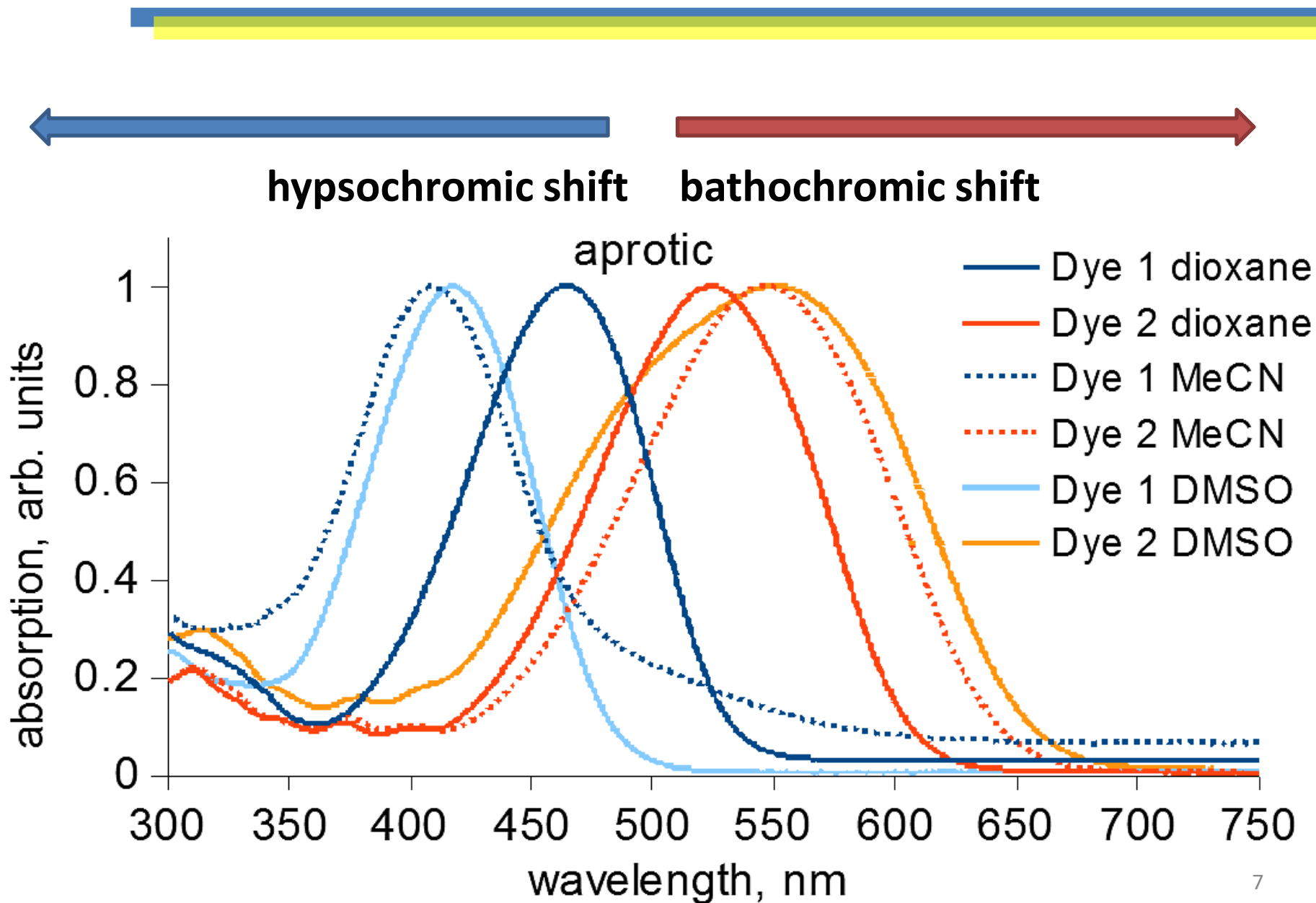


**FIGURE 13-4** Deviations from Beer's law with polychromatic radiation. The absorber has the indicated molar absorptivities at the two wavelengths  $\lambda'$  and  $\lambda''$ .

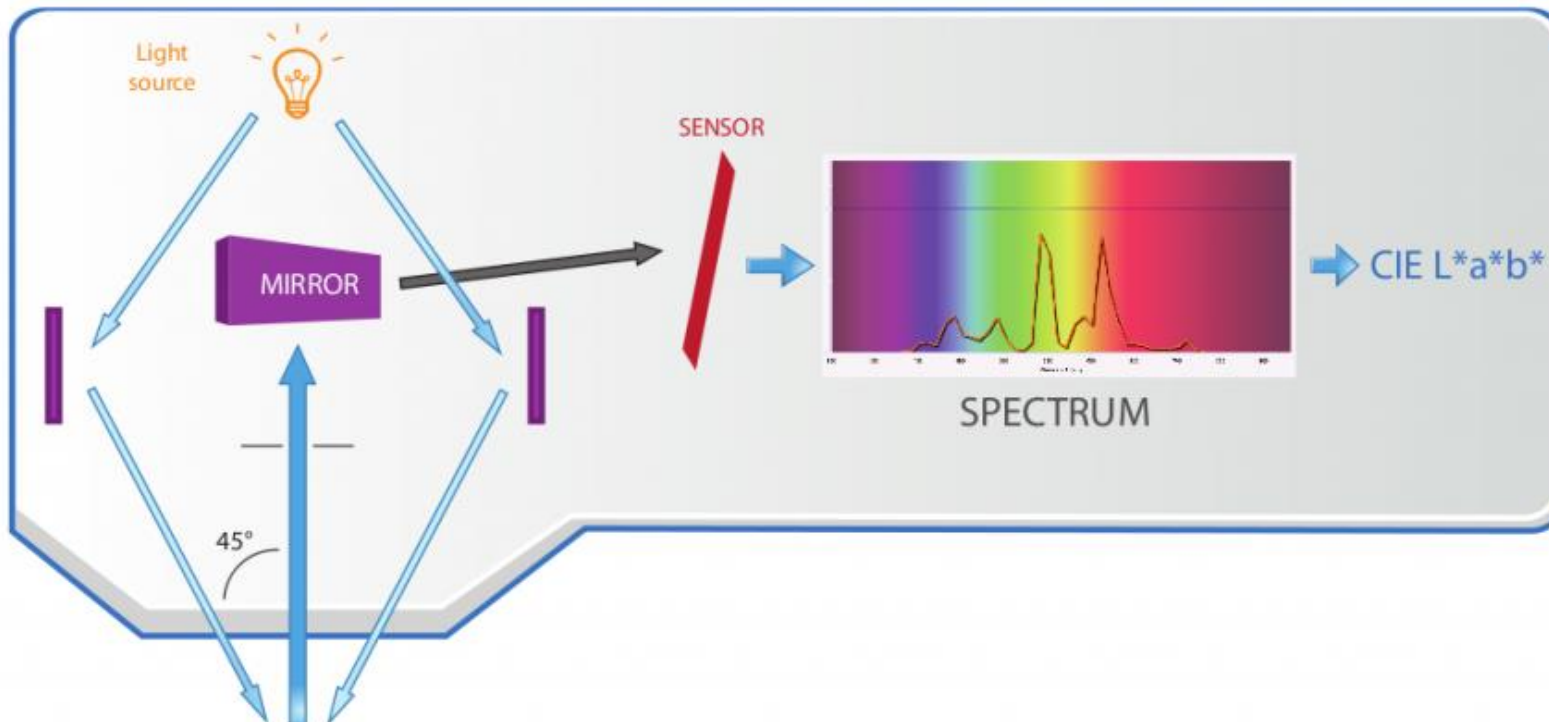
# Solvatochromism



# The Spectrophotometer

It is a colour measurement device that provides accurate readings about the current conditions of the press or computer screen

How does it work ?



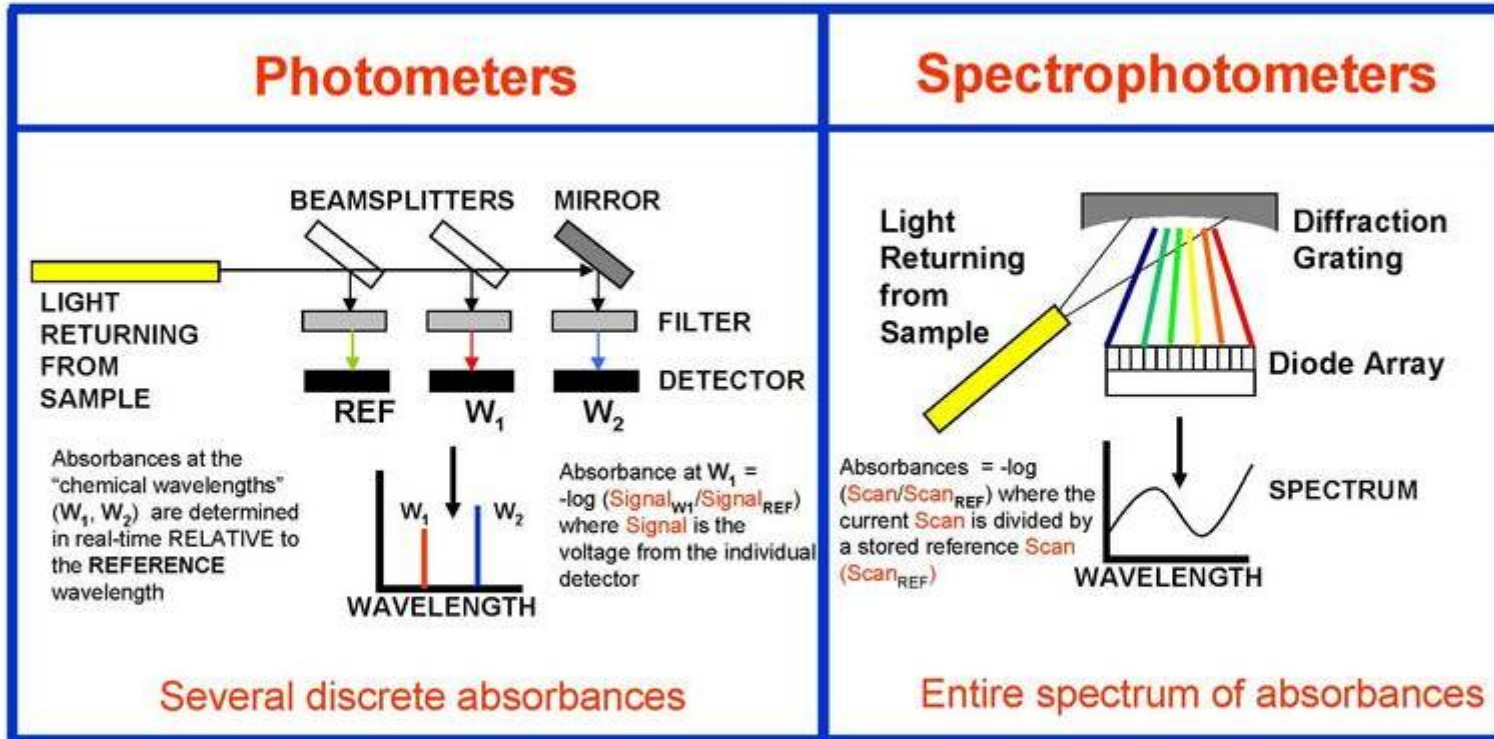
CHART



© Caldera. All rights reserved. Any reproduction in whole or in part on any medium or use of this graphic is prohibited without the prior written consent of Caldera.



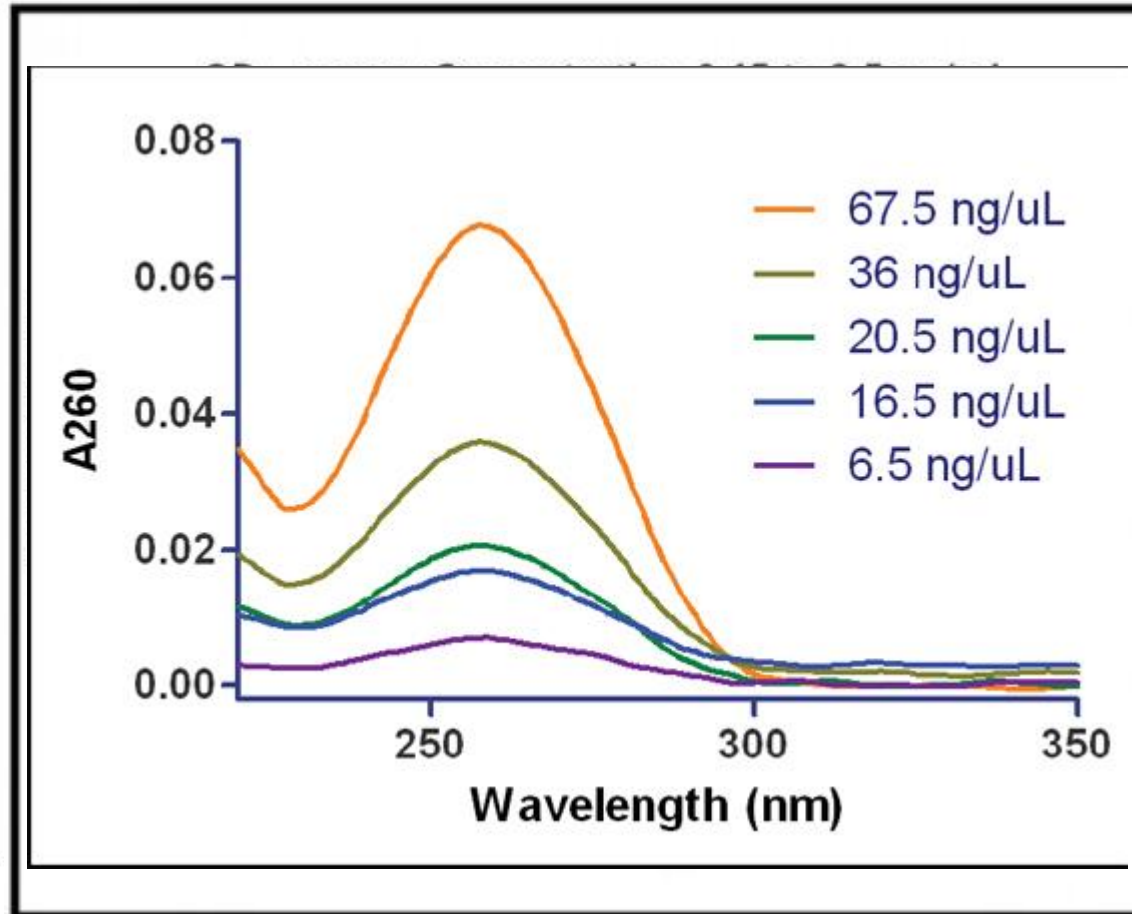
# How They Work



*Note: there are other methods, such as rotating filter wheel photometers and FT-NIR or rotating grating spectrophotometers*



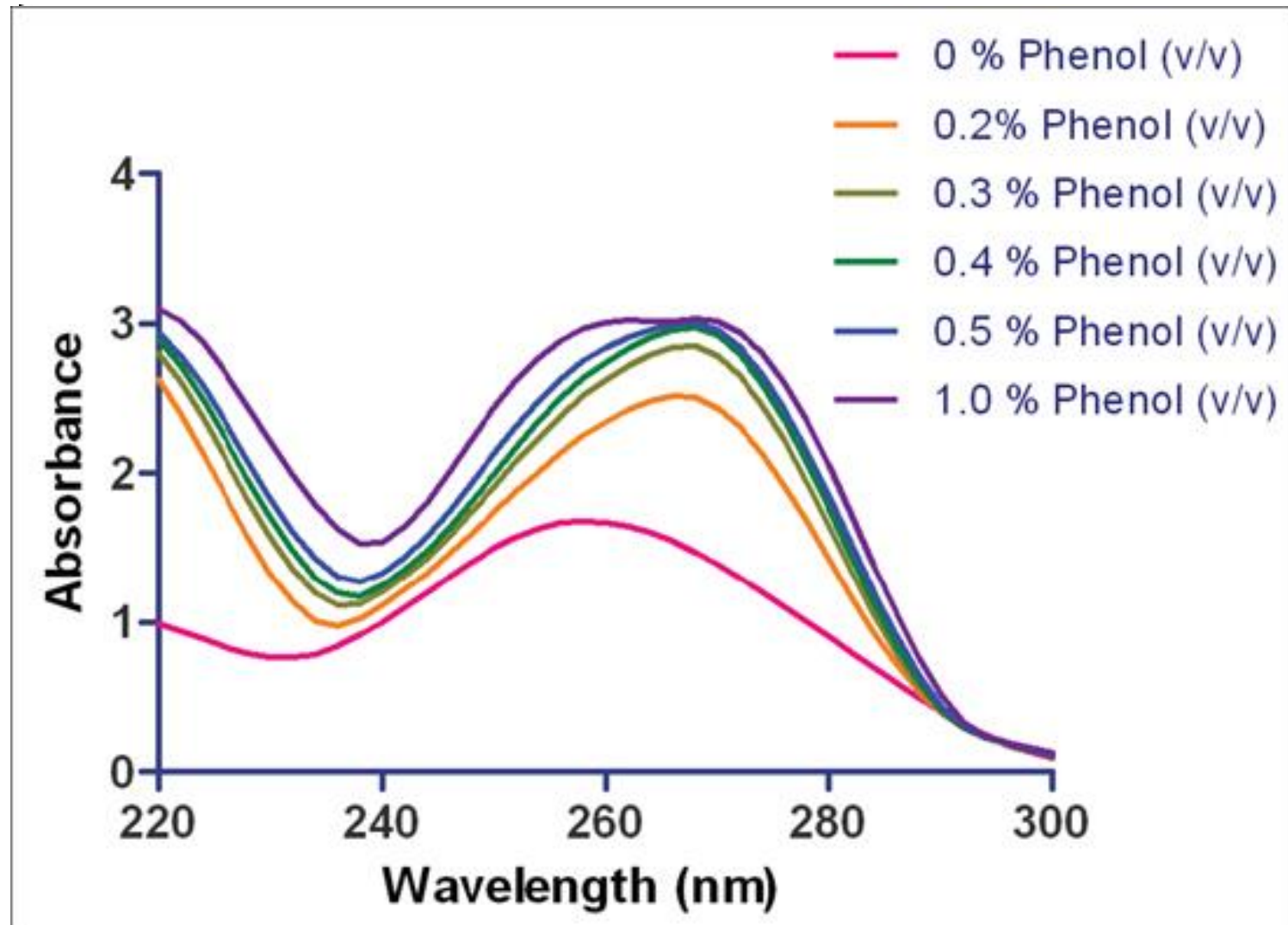
# Assays – DNA and proteins



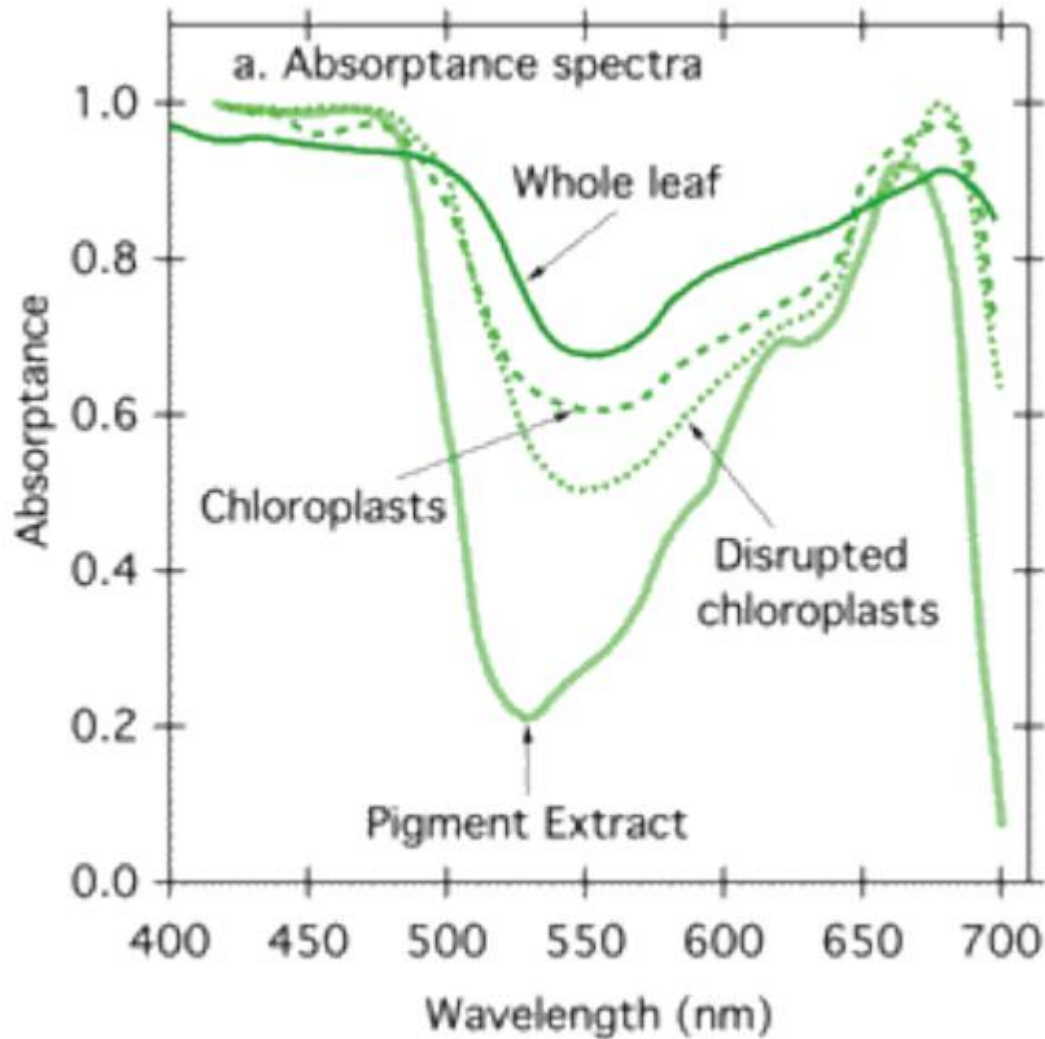
<http://oceanoptics.com/measuring-dna-absorbance-sts-uv-microspectrometer/>

<http://www.biotek.com/resources/articles/micro-volume-purity-assessment-nucleid-acids.html>

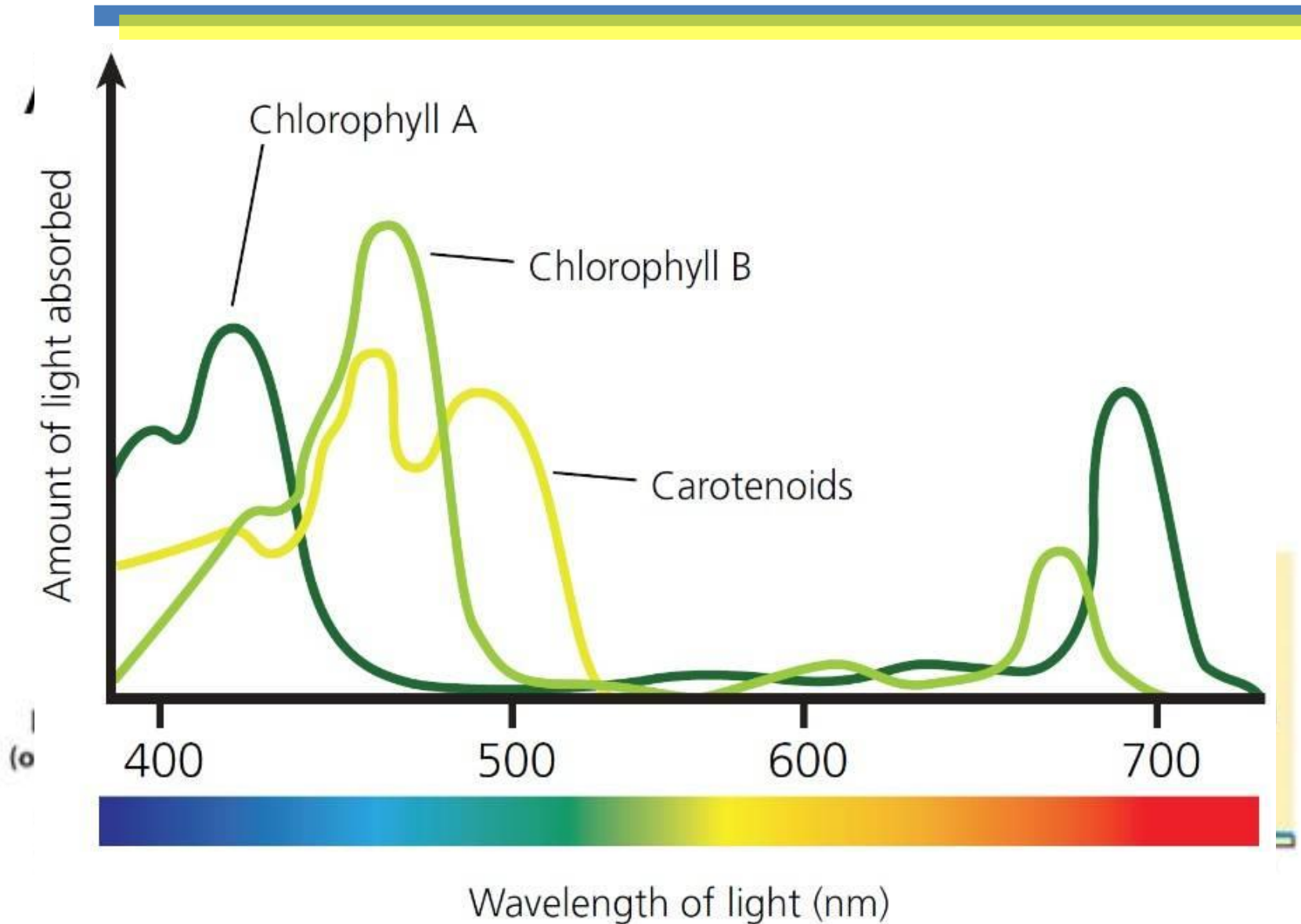
# Assays – DNA and proteins



# Mixing everything...



# Chemicals – some examples

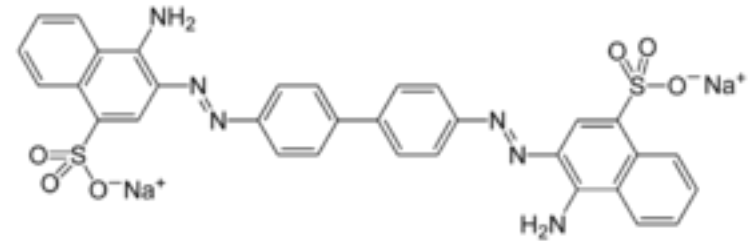
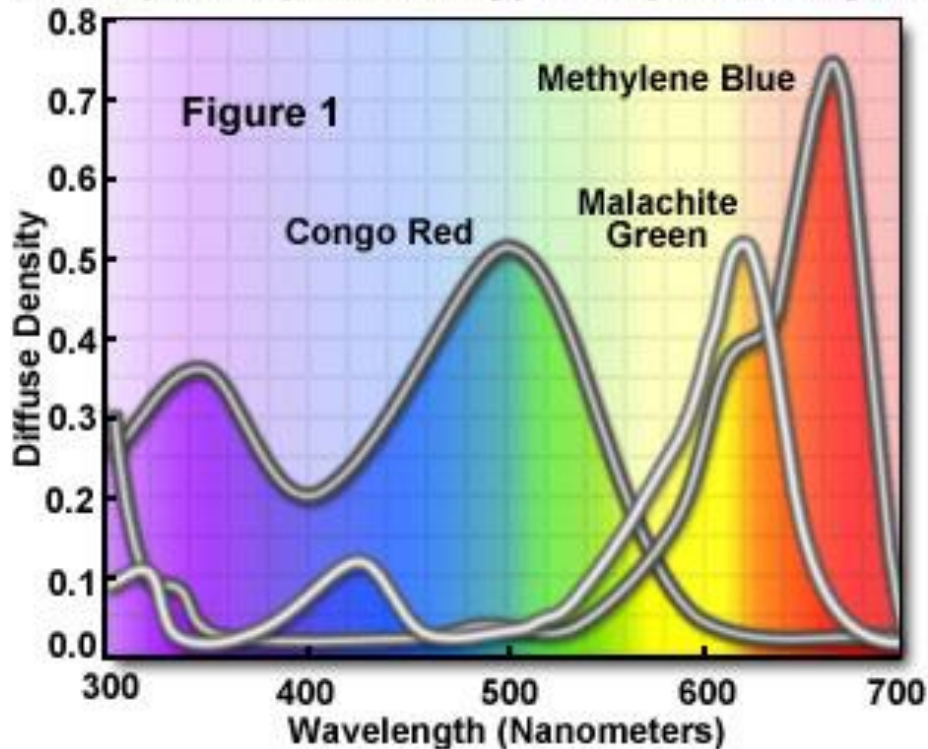


<http://pt.slideshare.net/codyalantaylor/spectrophotometry-lecture>

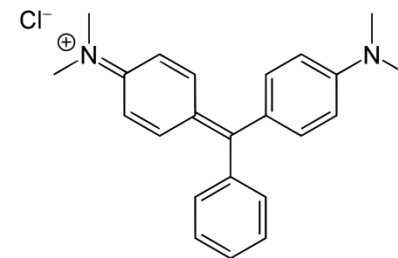
<https://www.heliospectra.com/blog/spectrum-101-absorption-spectra-versus-action-spectra>

# Molecular absorption of some biological stains

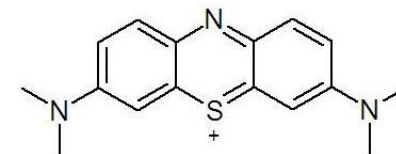
Figure 1  
Absorption Spectra of Typical Synthetic Dyes



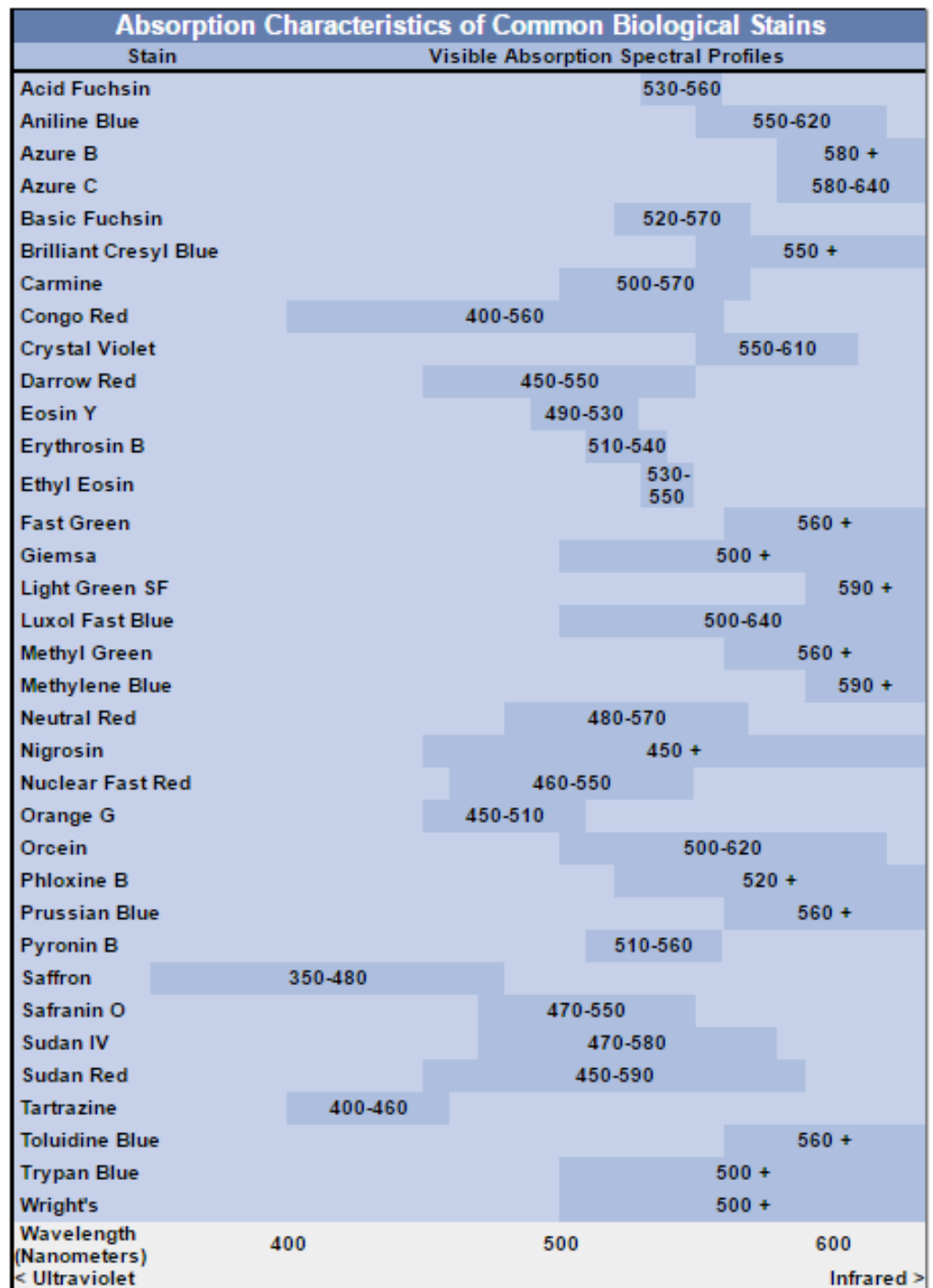
congo red



malachite green



methylene blue



<https://micro.magnet.fsu.edu/primer/photomicrography/bwstainchart.html>

# Colorimetric assays

---

- ✓ Tetrazolium salts
- ✓ Trypan blue
- ✓ Sulforhodamine B
- ✓ Neutral Red
- ✓ Resazurin - Alamar blue

...



# Tetrazolium salts

monotetrazolium salts are reduced by NAD(P)H-dependent oxidoreductases and dehydrogenases of metabolically active cells.

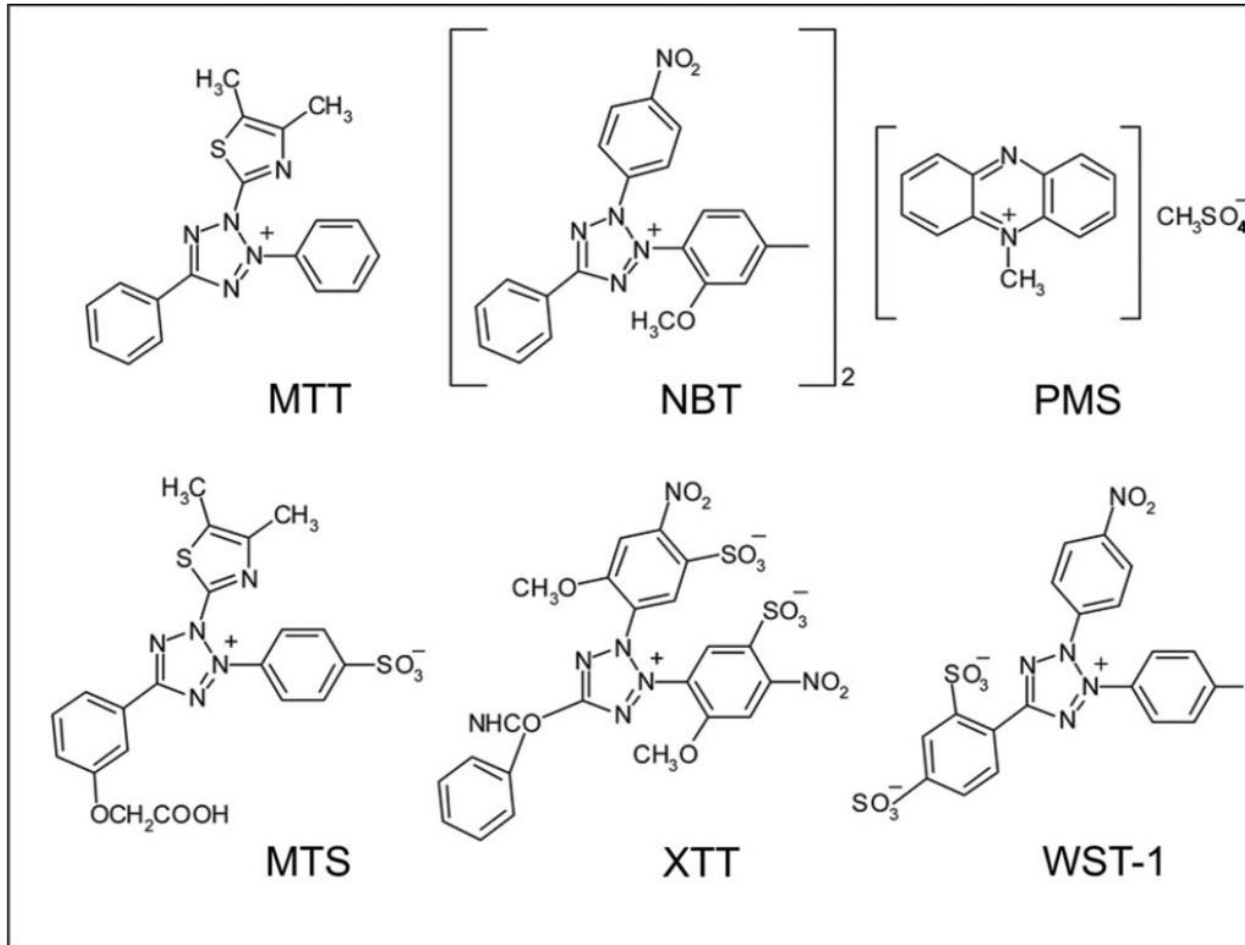


Fig. 1. Chemical structures of selected tetrazolium salts and of the intermediate electron acceptor, phenazine methosulfate (PMS).

Berridge, M.V.; Herst, P.M.;  
Tan, A.S.

Tetrazolium dyes as tools in  
cell biology: New insights  
into their cellular reduction.  
*Biotechnol. Ann. Rev.* **2005**,  
*11*, 127-152.

# Tetrazolium salts

reduction rates

MTT > MTS > XTT = WST-1

Studies also showed that MTT reduction does not correlate with DNA synthesis. 24h and above, it has some correlation with H<sup>3</sup>-thymidine (for DNA incorporation).

Superoxide does not cross de cell membrane

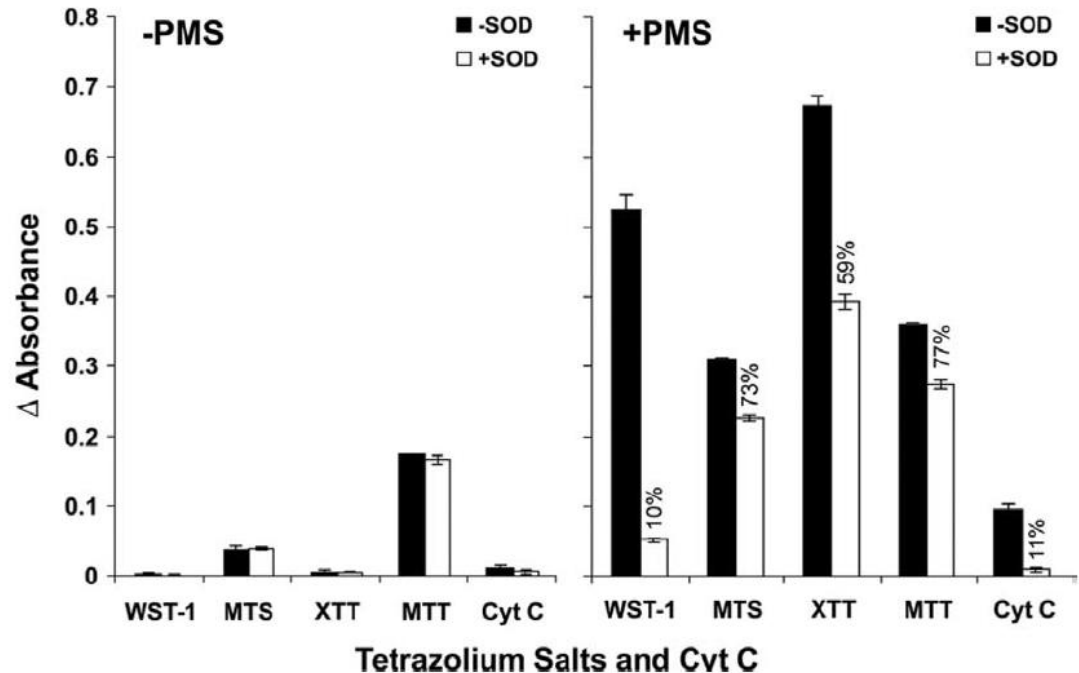
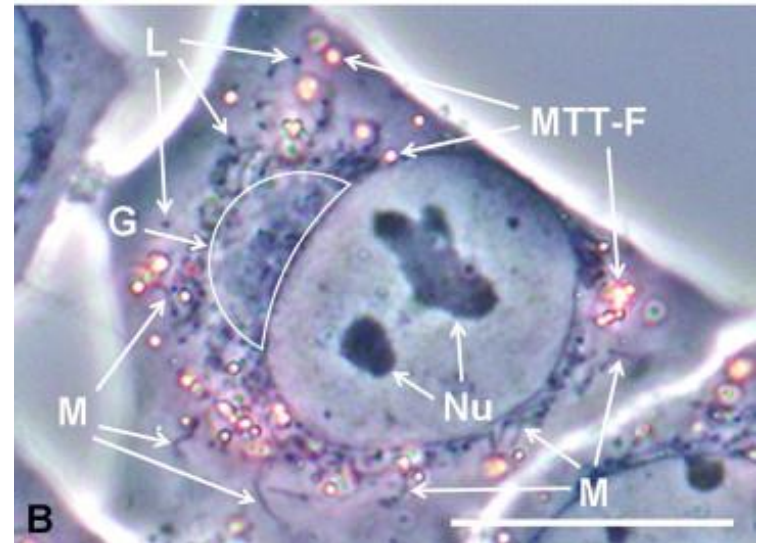
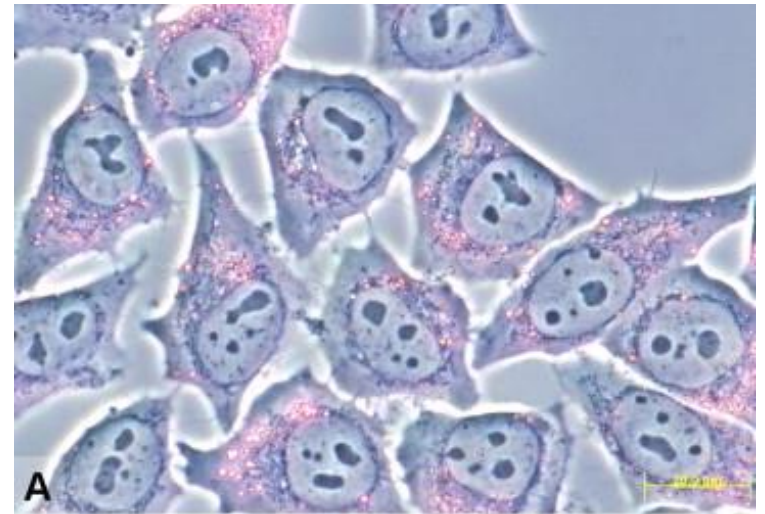
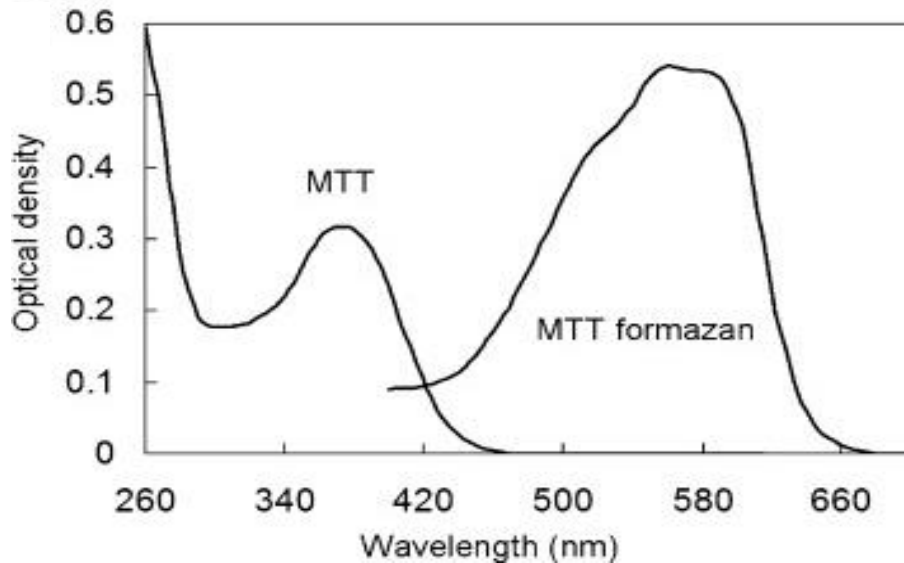
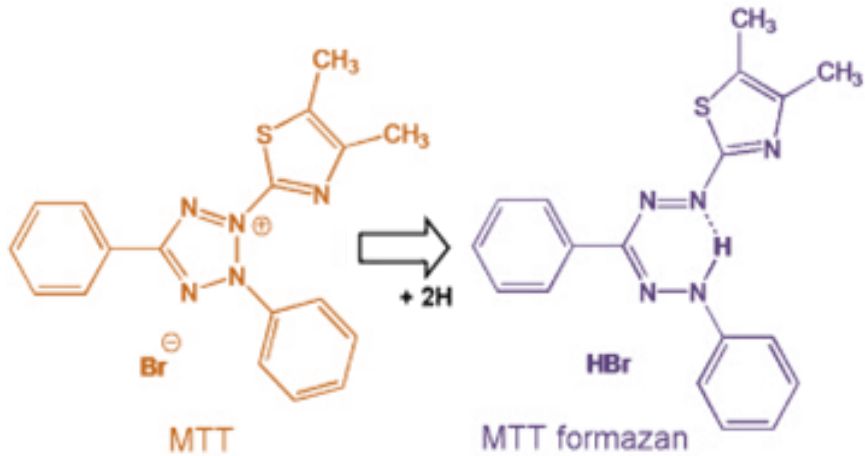


*Fig. 3.* Comparison of cellular tetrazolium dye reduction in the presence and absence of mPMS and SOD. Human T-lymphoblastic Jurkat cells ( $2-3 \times 10^4$  per microplate well) were incubated for 1 h with WST-1 (400  $\mu\text{g/ml}$ ), MTS (313  $\mu\text{g/ml}$ ), XTT (313  $\mu\text{g/ml}$ ), MTT (500  $\mu\text{g/ml}$ ) or ferricytochrome *c* (80  $\mu\text{M}$ ) in the presence and absence of mPMS (20  $\mu\text{M}$ ) and SOD (20  $\mu\text{g/ml}$ ). Absorbance was measured in a microplate reader at 450 nm for WST-1, MTS and XTT, 570nm for MTT and 550 nm for cytochrome *c*. SOD inhibition is presented as % control. Results are presented as the mean of duplicate determinations  $\pm$  standard error.

# MTT



Stockert, J. C.; Blázquez-Castro, A.; Cañete, M.; Horobin, R. W.; Villanueva, A. MTT assay for cell viability: Intracellular localization of the formazan product is in lipid droplets. *Acta Histochemica*, **2012**, *114*, 785–796

# MTT

**Table 1**  
**Interfering factors**

<b>Factor</b>	<b>Type of interference</b>	<b>Solution</b>
Glucose	Lack of glucose lowers MTT production through decreased glycolysis	Do not use exhausted medium (change it few hours before assay)
Protein precipitation	Organic solvents may cause precipitation of serum proteins, which interferes with the reading	Use different solvent
Phenol red	Phenol red interferes with reading, its absorbance is pH-dependent	Use acidified solvent or medium without phenol red
Incomplete solubilization	Formazan crystals do not dissolve, and this lowers the sensitivity of the assay	Increase shaking intensity and/or extraction time
Confluency	(Over)confluent cells may lower their metabolic rate, resulting in underestimation of cell number	Use lower initial seeding density if possible
Metabolic rate	The metabolic rate of the cells is changed by the treatment	Use standard curve for each treatment, or find alternative cell counting method

# WST

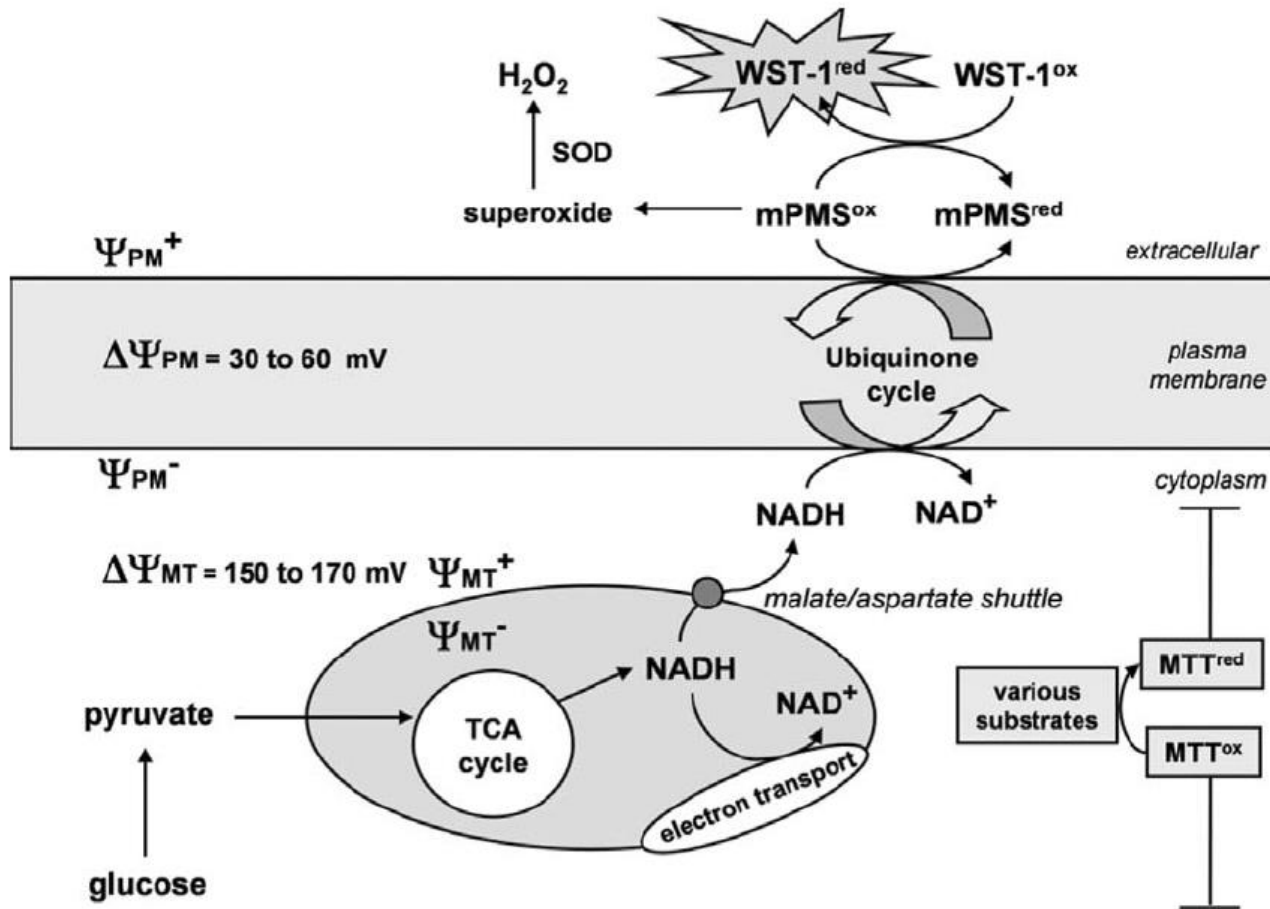
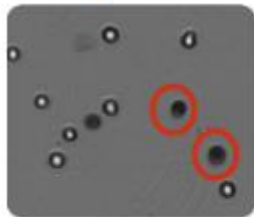
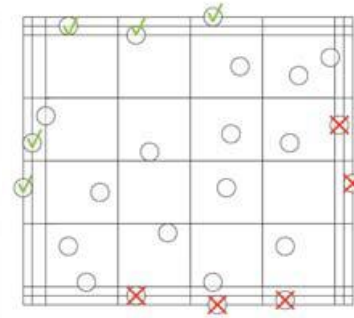
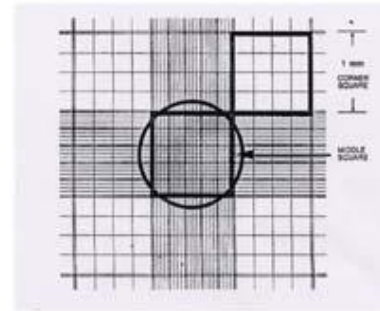
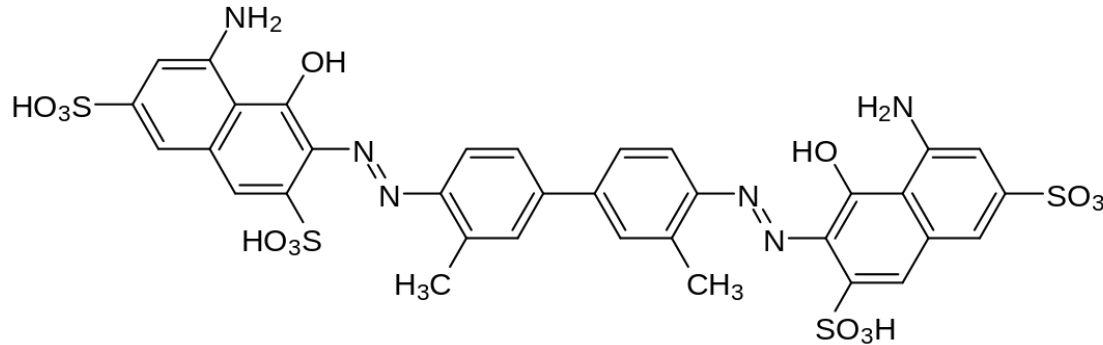


Fig. 2. Schematic representation of the proposed mechanisms of cellular reduction of MTT and WST-1. Whereas MTT is reduced by a variety of intracellular reductants, most notably NADH, WST-1 is reduced by trans-plasma membrane electron transport via the electron carrier, 1-methoxyPMS, in which case the cellular reductant is NADH derived mainly from the mitochondrial TCA cycle. The plasma membrane potential, which is proposed to be the major cellular determinant of tetrazolium dye uptake is also depicted.

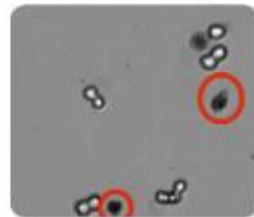
# Trypan blue

Colorimetric method for the analysis of cell viability.

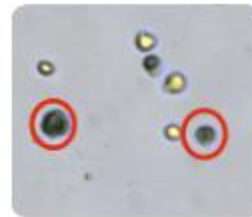
Incorporation of the dye means cell death due to membrane disruption.



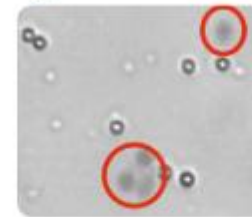
Jurkat cells imaged  
by Cellometer  
Vision



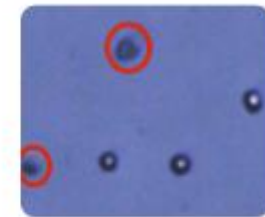
CHO cells imaged  
by Cellometer  
Vision



HeLa cells imaged  
by Cellometer Auto  
T4



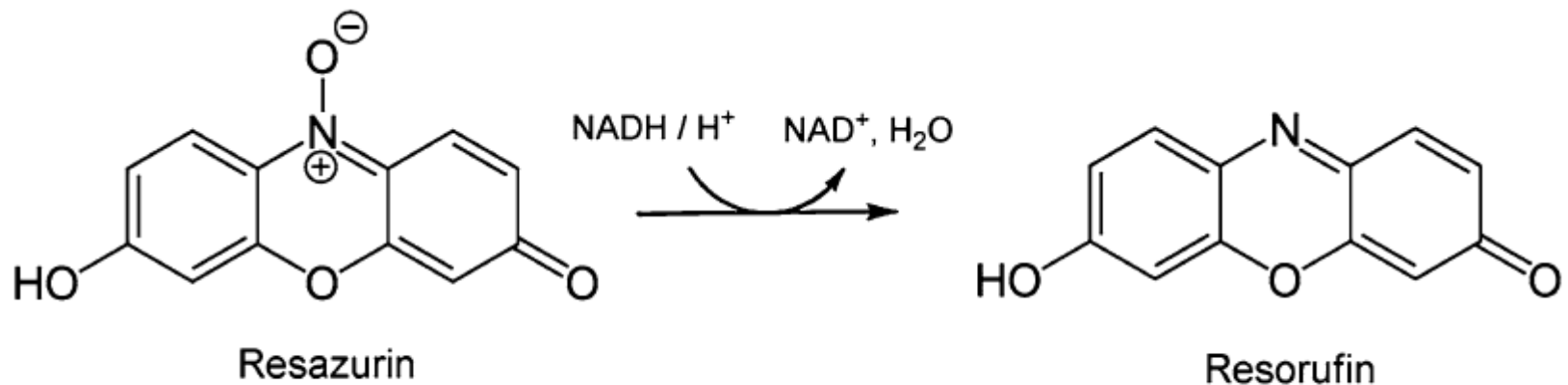
Splenocytes  
imaged by  
Cellometer Auto  
2000



Jurkat cells imaged  
by Cellometer Auto  
1000

More recently: use of this dye as a fluorescent marker.

# Resazurin



Mechanism of reduction of resazurin to resorufin.

# Resarzurin- Alamar blue

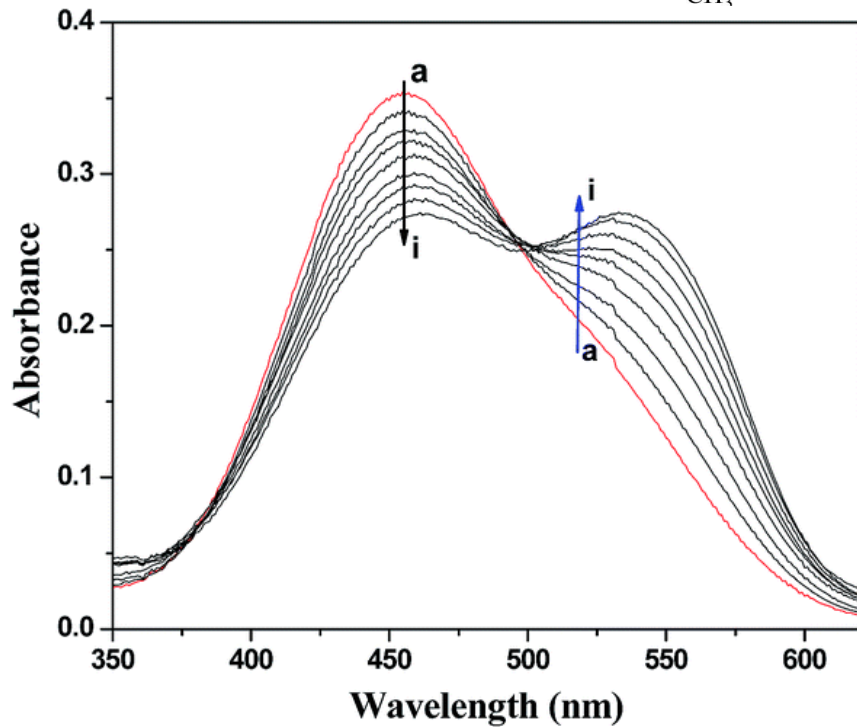
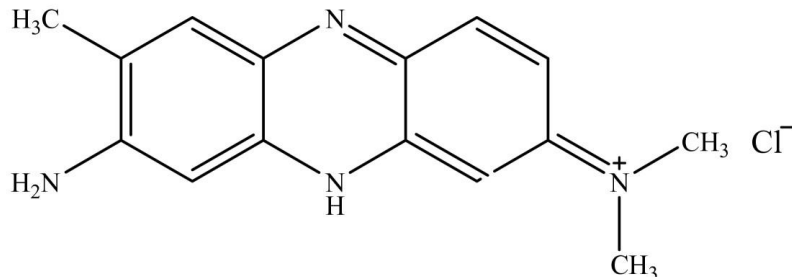
**Table 1**

**The recommended conditions for the Alamar Blue assay in 96-well plate for normal and cancer cell lines. Reprinted from (14) with permission from Elsevier**

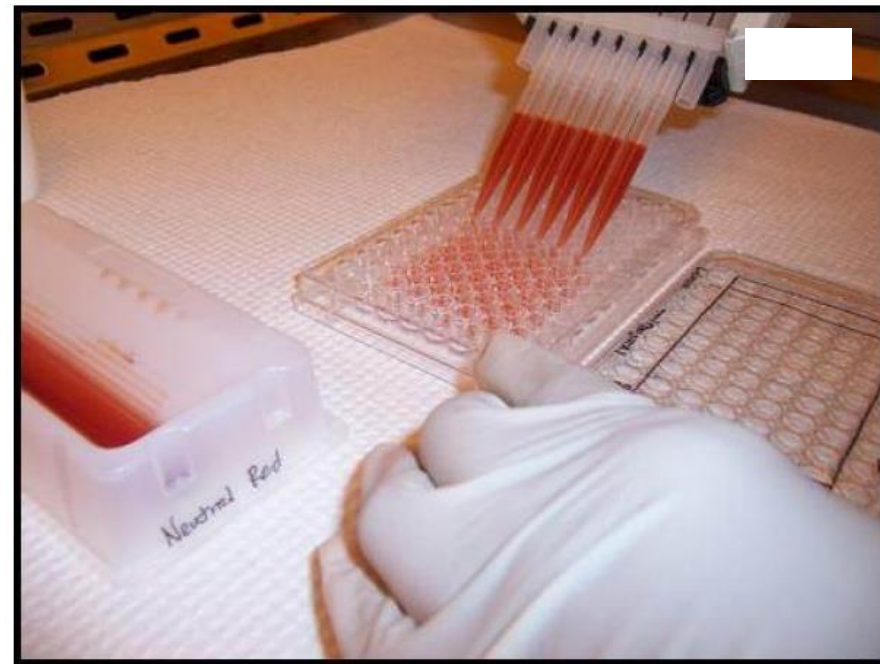
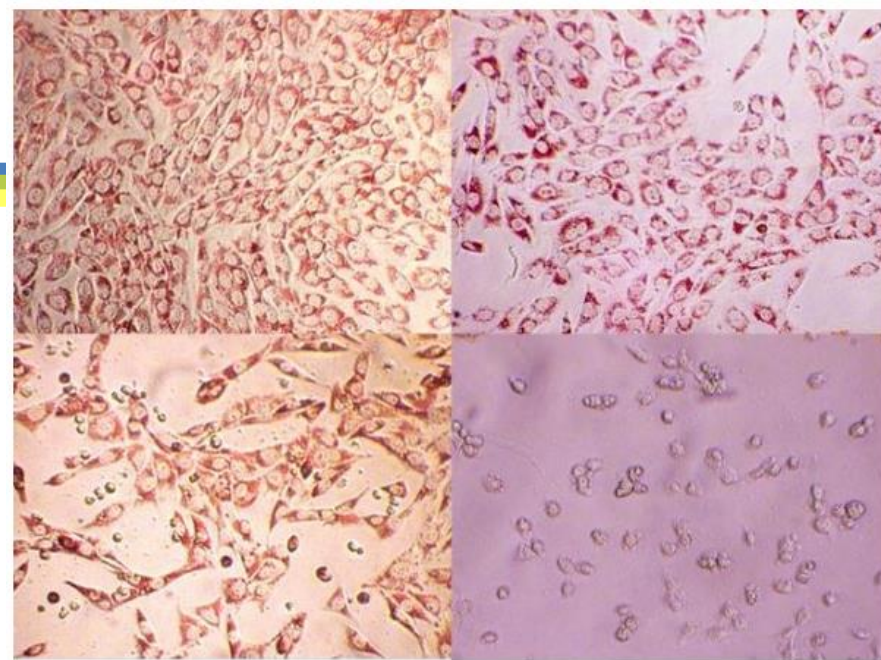
<b>Cell line</b>	<b>Linear range (cell number <math>\times 10^4</math>)</b>	<b>Optimal AB concentration (%)</b>	<b>Optimal incubation time (h)</b>
<b>Normal cell lines</b>			
BALB/3T3	0.05–2	4	3
CHO-K1	0.05–3	10	3
NJTIDF 4054	0.05–2	4	3
<b>Ovarian cancer cell lines</b>			
2008	0.05–3	4	1
IGROV-1	0.05–3	10	1
OVCAR-3	0.05–3	4	3
SK-OV-3	0.05–3	4	3
<b>Leukaemia cell lines</b>			
HL-60	0.5–5	10	6
K-562	0.5–5	10	6
MOLT-4	0.5–5	10	6



# Neutral red

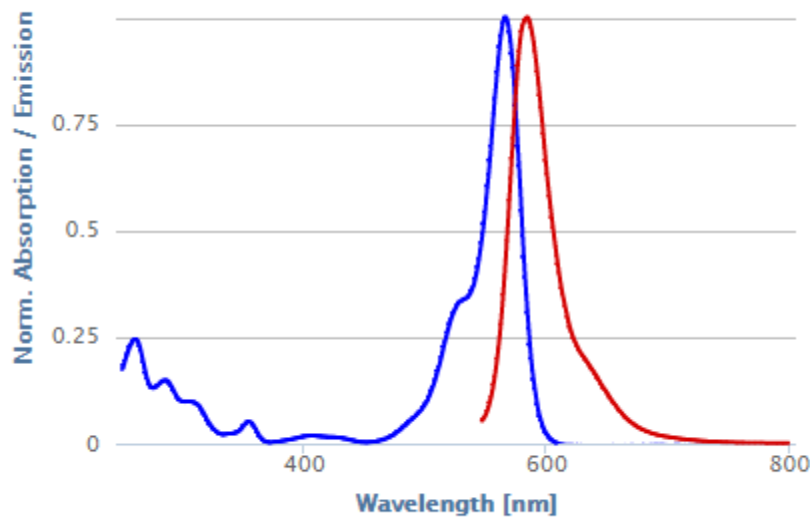
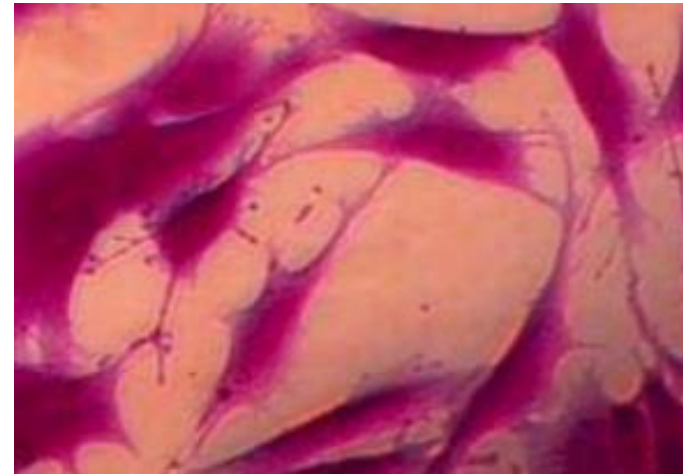
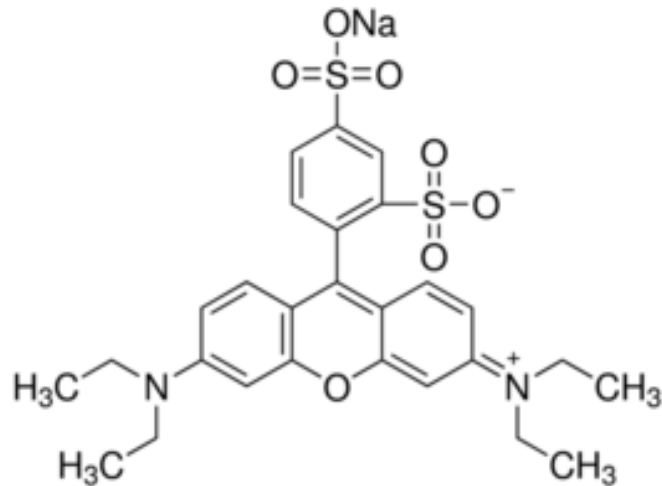


UV absorption spectra of NR in the presence of DNA at pH 7.4 and room temperature. [NR] = 20  $\mu\text{M}$ ., [DNA] = 0–52,5  $\mu\text{M}$ .  
Ref: *Med. Chem. Commun.*, 2015,6, 222-229



Neutral Red Addition: Neutral red is added to the 96-well plate.

# Sulforhodamine B



## Overview

Absorption  $\lambda_{\max}$

**566 nm, 355 nm**

Emission  $\lambda_{\max}$

**584 nm**

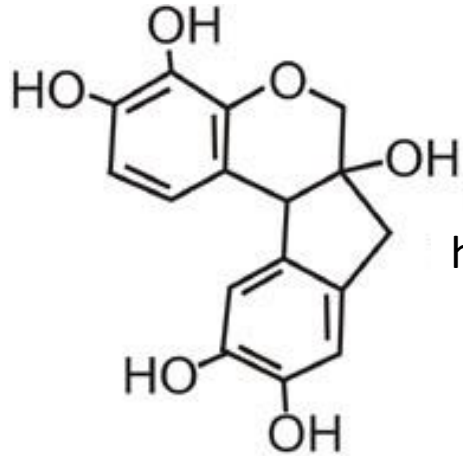
Solvent

**water**

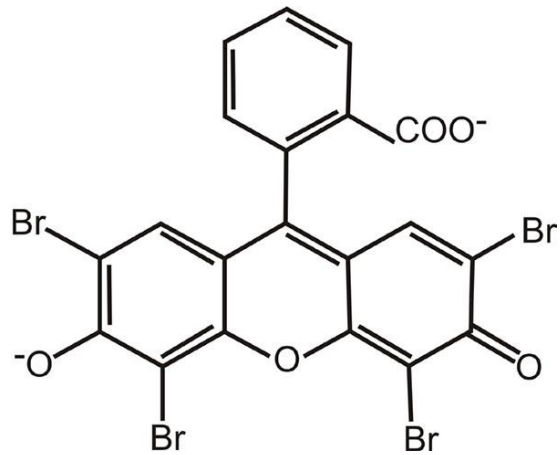
Molar Abs. Coefficient

-

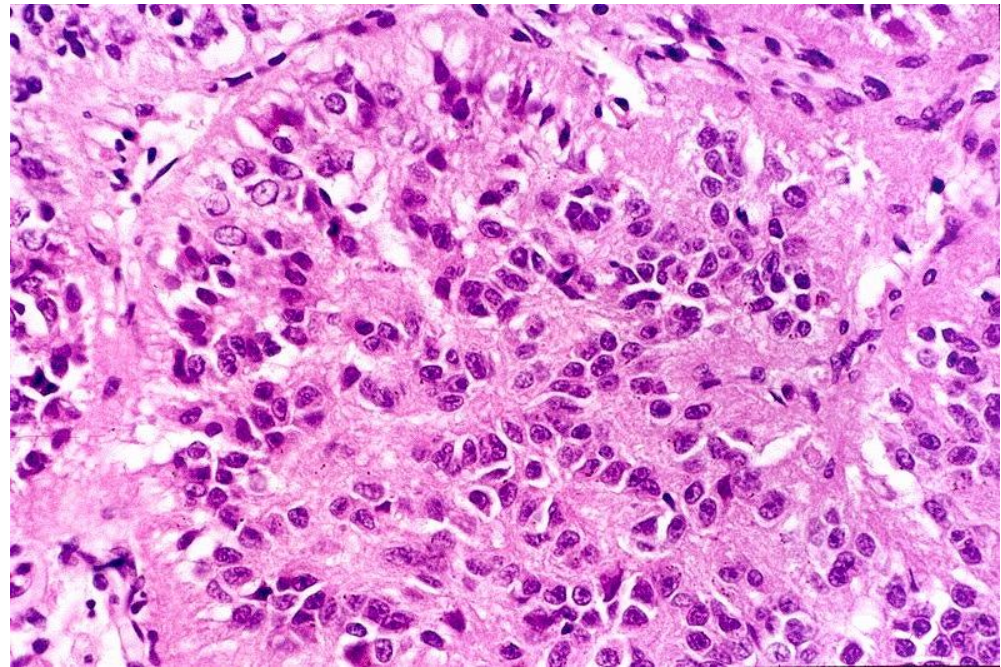
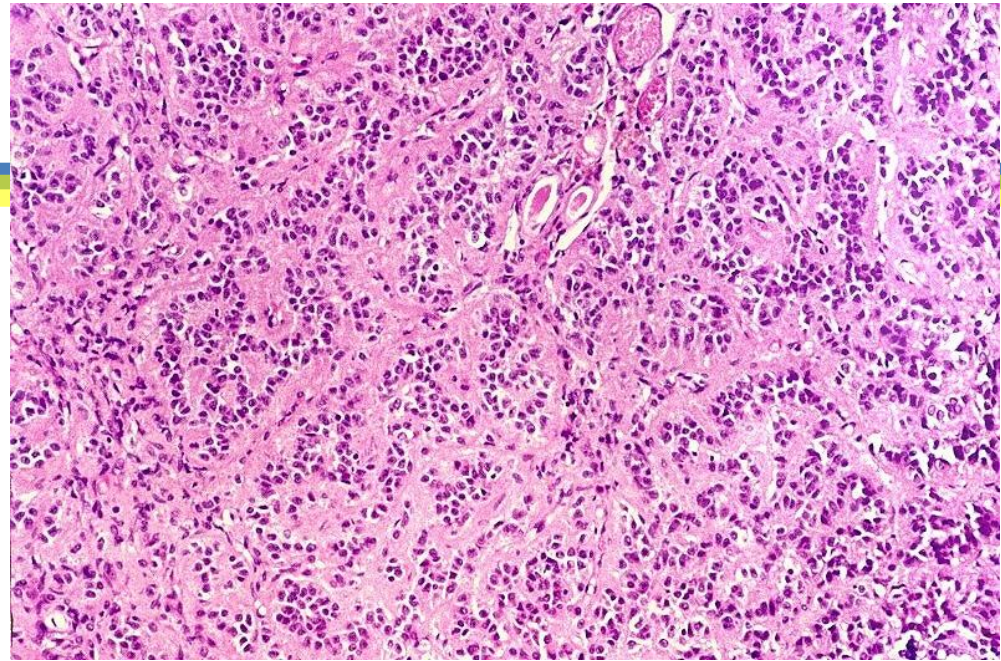
# Hematoxylin-eosin



hematoxylin



eosin



# Label-free technologies

# Impedance

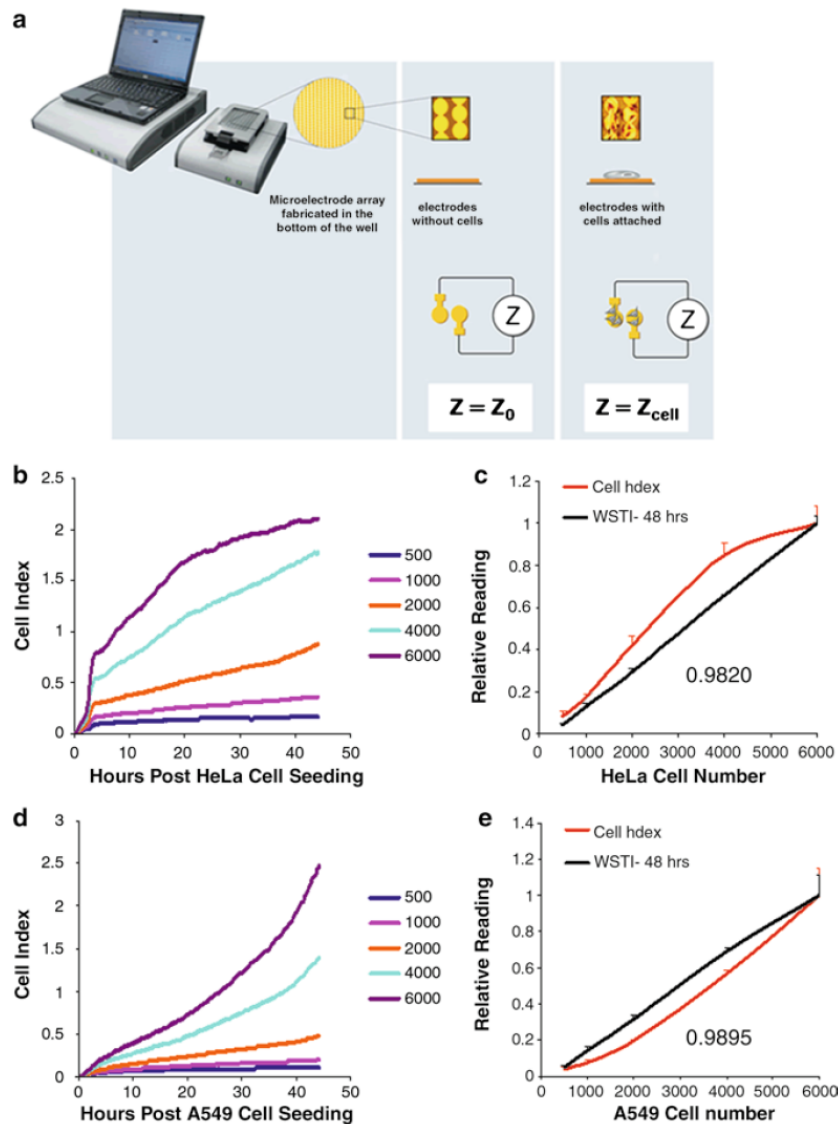


Fig. 1. xCELLigence in real-time monitoring of cell proliferation. (a) RTCA-SP instrument is shown, consisting of control unit, station, E-Plate, and display unit. Interdigitated gold electrodes at the bottom of the E-Plate are shown with or without cells. Background impedance is determined for medium alone ( $Z_0$ ), then after the cells attach and proliferate on the electrodes ( $Z_{\text{cell}}$ ). (b–e) Different numbers of HeLa (b) and A549 (d) cells were seeded in the E-Plate and the cell index was continuously monitored for 45 h. At the end of study, WST-1 was added to the medium and absorbance determined (c and e). Both cell index and WST-1 readings at the end of study were normalized against the value obtained at the highest seeding density. The average of triplicate samples is plotted with error bars indicating standard deviation. The Pearson correlation coefficient between WST-1 and cell index readings is also indicated.

Ning Ke, Xiaobo Wang, Xiao Xu, and Yama A. Abassi. The xCELLigence System for Real-Time and Label-Free Monitoring of Cell Viability. Chapter 6. Martin J. Stoddart (ed.), *Mammalian Cell Viability: Methods and Protocols*, Methods in Molecular Biology, vol. 740, DOI 10.1007/978-1-61779-108-6\_5, © Springer Science+Business Media, LLC 2011

# Label-free technologies

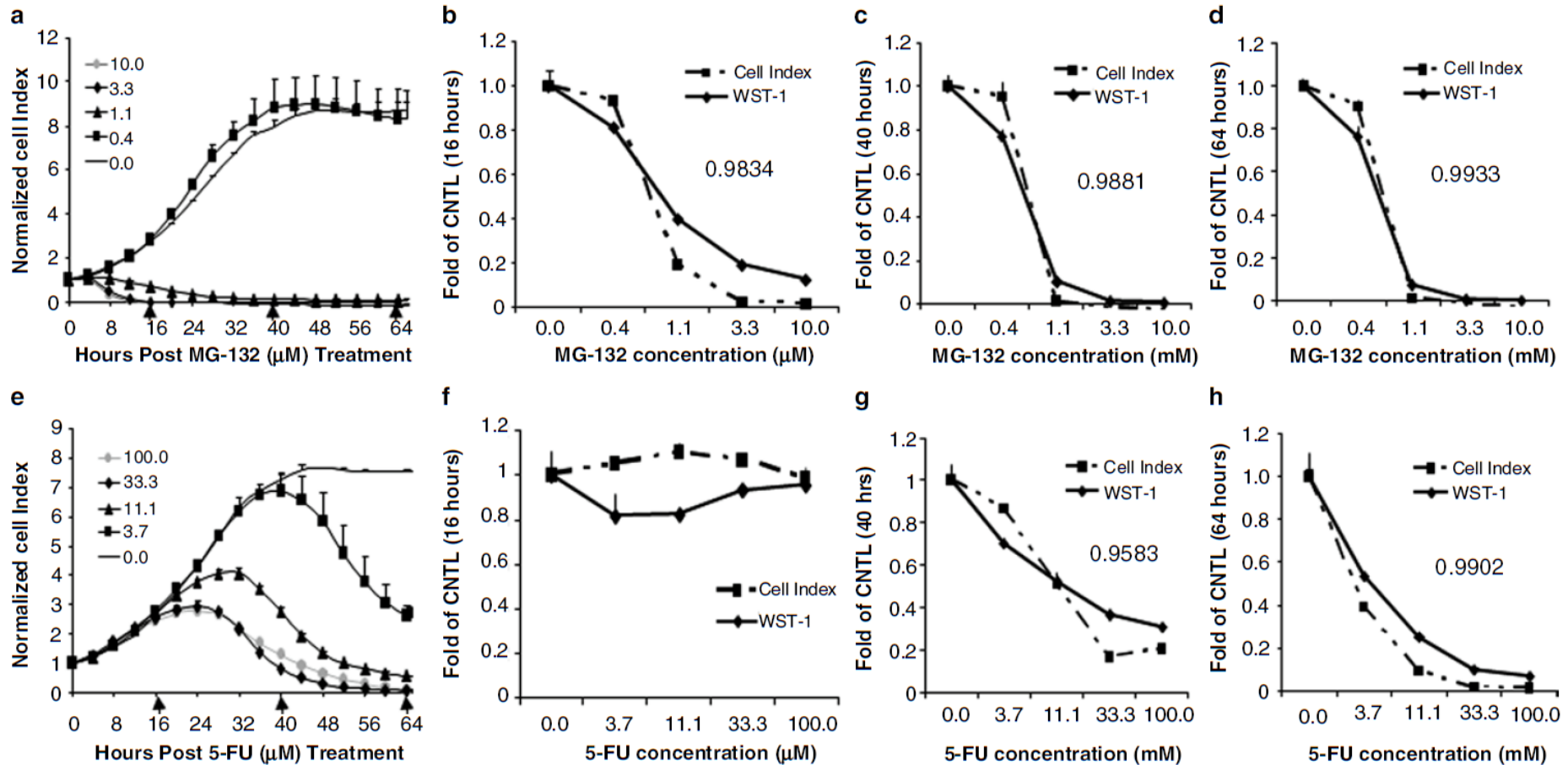


Fig. 2. xCELLigence system allows real-time monitoring of cell viability. HeLa cells were treated with various concentrations of the proteasome inhibitor MG-132 (**a–d**) and the DNA-damaging agent 5-FU (**e–h**). Cell index was monitored continuously for 64 h and the normalized cell index was derived by dividing the cell index value at each time point by the cell index at time of compound additions and plotted (**a** and **e**). No compound (no cpd) was used as control. Parallel experiments were also set up in E-plates for the WST-1 assay, which was performed at 16, 40, and 64 h post compound addition (**b–d** and **f–h**). Normalized cell index and WST-1 readings against control samples (untreated) were shown at the respective time points (16 h, **b** and **f**; 40 h, **c** and **g**; 64 h, **d** and **h**). The average of triplicate samples was shown and the error bars indicate standard deviation. The Pearson correlation coefficient was also shown for each case where cytotoxicity was observed.

# Label-free technologies

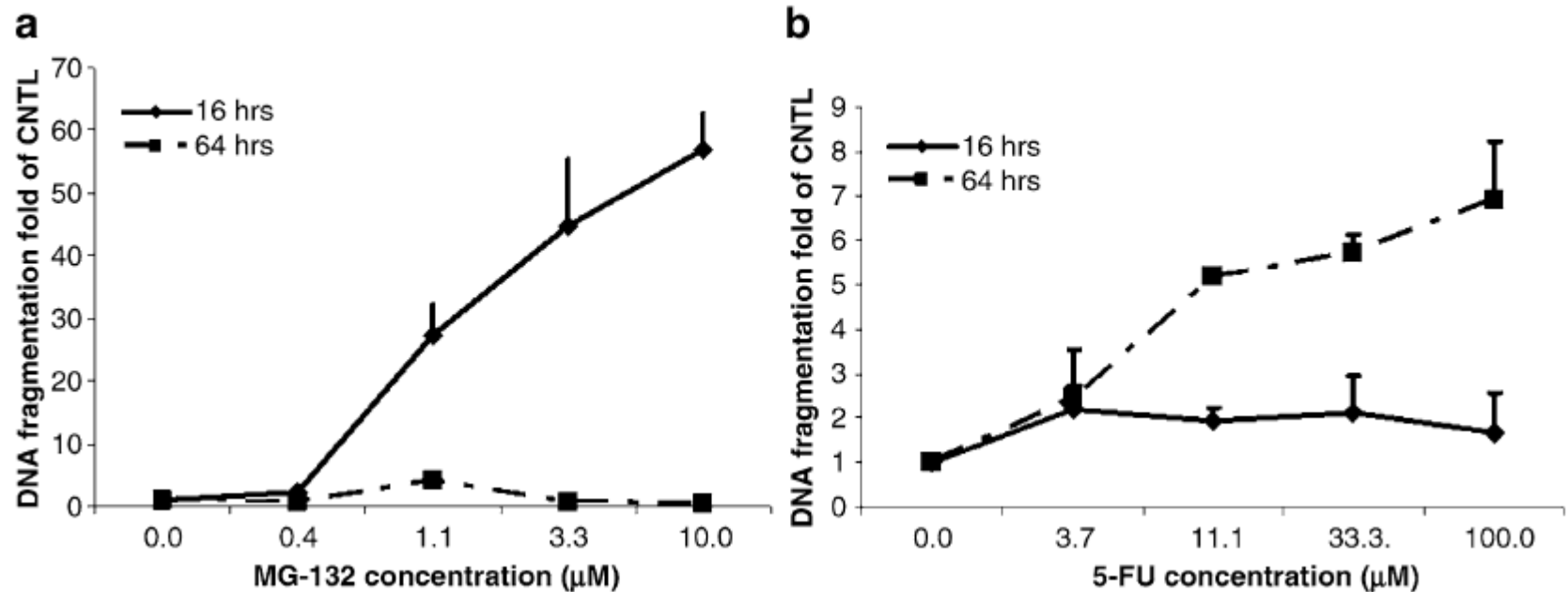


Fig. 3. Cell index changes and apoptosis. HeLa cells were treated with various concentrations of the proteasome inhibitor MG-132 (a) and the DNA-damaging agent 5-FU (b) and the cell index was monitored continuously for 64 h as in Fig. 2. A parallel experiment was set up in an E-plate and samples were harvested at 16 (solid line) and 64 h (dotted line) post compound addition for apoptosis assays (a and b). Apoptosis was determined using Cell Death Detection Elisa-Plus kit, and was expressed as the ratio of DNA fragmentation signal to that of the untreated samples. While the proteasome inhibitor MG-132 exerts its effect on cell index as early as 4 h post treatment, with maximal effect at 10 h post treatment, 5-FU effect is much slower, with onset at ~16 h post treatment, and the maximal effect observed after 48 h. Correspondingly, apoptosis induction is observed at 16 h for MG-132, and at 64 h for 5-FU. Importantly, no apoptosis induction is observed for MG-132 at 64 h, confirming the transient nature of apoptosis and indicating the importance of continuous monitoring of cell viability in selecting optimal time points for end-point assays.

# Microcalorimetry

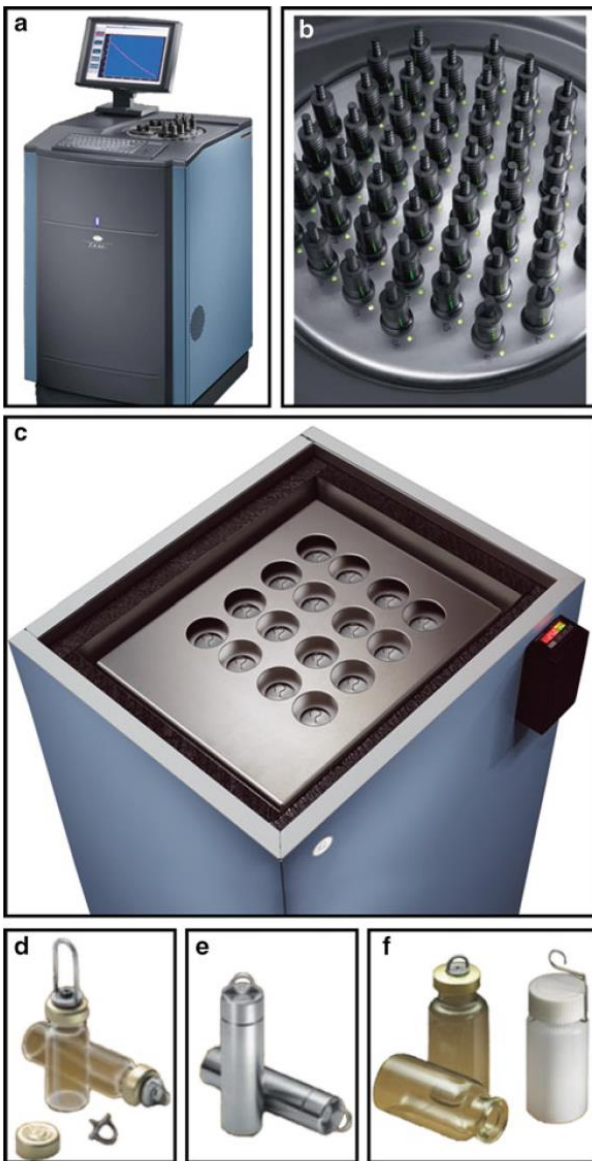


Fig. 1. Examples of commercially available isothermal microcalorimetry (IMC) instruments with multiple microcalorimeters or calorimeters, and ampoules for closed ampoule studies. All instruments and ampoules: Waters/TA, New Castle DE USA (images: courtesy of Waters/TA) (a) General view of a TAM III<sup>®</sup> equipped with various microcalorimeters. (b) Top view of a TAM 48<sup>®</sup> with its array of 48 microcalorimeters (i.e. 48 individual measuring channels). (c) Top view of a TAM Air<sup>®</sup> showing its eight individual differential calorimeters. (d) 3- and 4-ml disposable glass ampoules. (e) 4-ml stainless steel ampoules. (f) 20-ml disposable glass and polyethylene ampoules.

Olivier Braissant and Alma U. Daniels. Closed Ampoule Isothermal Microcalorimetry for Continuous Real-Time Detection and Evaluation of Cultured Mammalian Cell Activity and Responses. Chapter 20

Martin J. Stoddart (ed.), *Mammalian Cell Viability: Methods and Protocols*, Methods in Molecular Biology, vol. 740, DOI 10.1007/978-1-61779-108-6\_5, © Springer Science+Business Media, LLC 2011



# Microcalorimetry

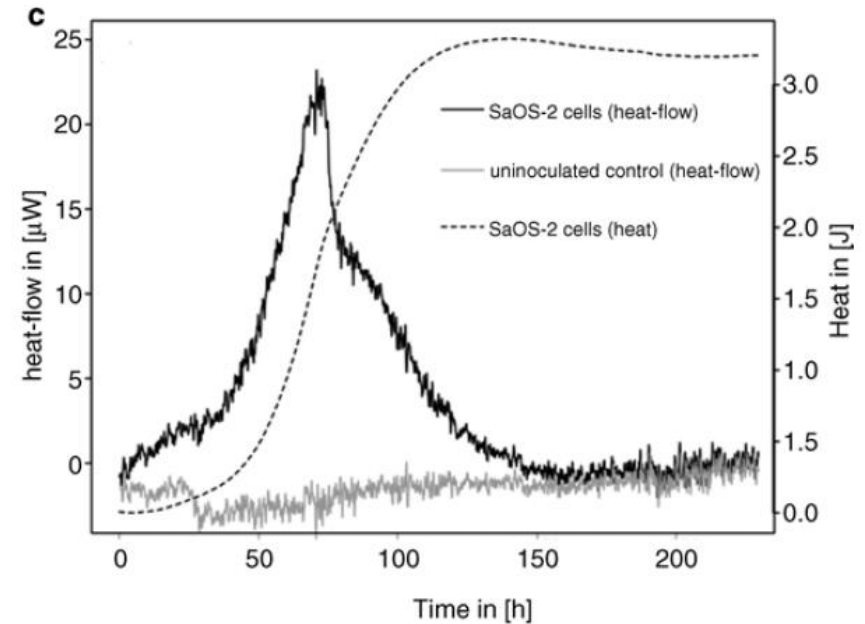
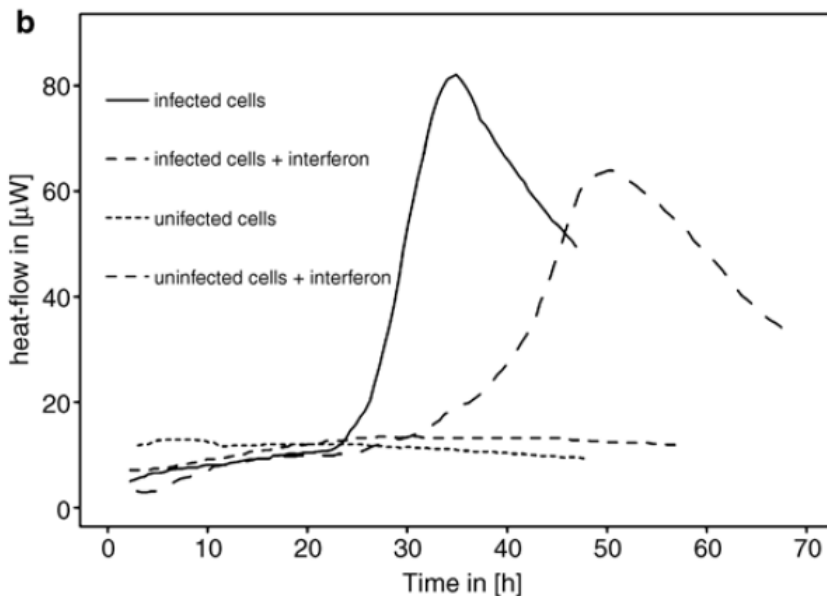
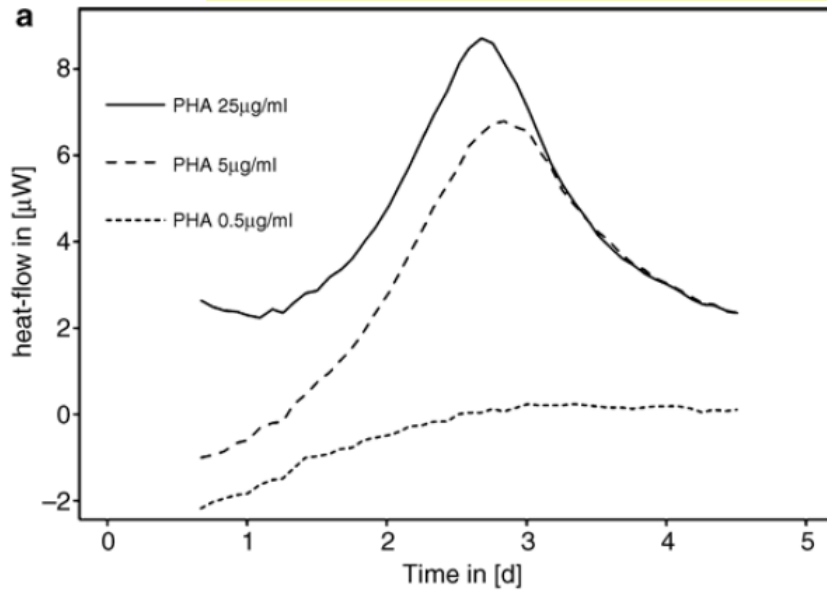


Fig. 4. Examples of heat flow data obtained following protocols. (a) Monitoring lymphocyte activity showing heat flow from lymphocytes (initial amount  $2.5 \times 10^5$  cells) over a period of days when stimulated with various amounts of phytohemagglutinin (PHA).

(b) Monitoring virus infection in mammalian cells, showing heat flow from BHK-21 cells at 37°C. (a) FMDV infected cells (*plain line*), (b) infected cells with 1.0 mg/ml interferon (*dashed line*), (c) uninfected cells with 1.0 mg/ml interferon (*dashed line*), and (d) uninfected cells without interferon (*dashed line*). (c) Monitoring growth of SaOS-2 (human sarcoma osteogenic) cells (authors' data). *Plain dark line*: cells in culture, *Plain grey line*: inoculated control, *dashed line*: accumulated heat (J) vs. time, base on heat flow curve obtained during growth. Accumulated heat vs. time is analogous to conventional growth curves showing, e.g. the accumulated number of cells.